clean technologies

MDPI

Article

Mathematical Modeling of Particle Terminal Velocity for Improved Design of Clarifiers, Thickeners and Flotation Devices for Wastewater Treatment

Dario Friso [1,2]

[1] Campus of Agripolis, University of Padova, Via dell'Università, 16, 35020 Legnaro, Italy; dario.friso@unipd.it
[2] MATHERES—Mathematical Engineering Research, Via Misurina, 1, 35035 Mestrino, Italy

Abstract: The prediction of the terminal velocity of a single spherical particle is essential to realize mathematical modeling useful for the design and adjustment of separators used in wastewater treatment. For non-spherical and non-single particles, terminal velocity can be traced back to that of single spheres using coefficients and Kynch's theory, respectively. Because separation processes can involve small or large particles and can be carried out using gravity, as with clarifiers/thickeners, or by centrifugation in centrifuges where the acceleration can exceed 10,000$\times$ g, the Reynolds number of the particle can be highly variable, ranging from 0.1 to 200,000. The terminal velocity depends on the drag coefficient, which depends, in turn, on the Reynolds number containing the terminal velocity. Because of this, to find the terminal velocity formula, it is preferable to look first for a relationship between the drag coefficient and the Archimedes number which does not contain the terminal velocity. Formulas already exist expressing the relationship between the drag coefficient and the Archimedes number, from which the relationship between the terminal velocity and the Archimedes number may be derived. To improve the accuracy obtained by these formulas, a new relationship was developed in this study, using dimensional analysis, which is valid for Reynolds number values between 0.1 and 200,000. The resulting mean relative difference, compared to the experimental standard drag curve, was only 1.44%. This formula was developed using the logarithms of dimensionless numbers, and the unprecedented accuracy obtained with this method suggested that an equally accurate formula for the drag coefficient could also be obtained with respect to the Reynolds number. Again, the resulting level of accuracy was unprecedentedly high, with a mean relative difference of 1.77% for Reynolds number values between 0.1 and 200,000.

Keywords: wastewater treatment; clarifiers; thickeners; flotation devices; design; mathematical modelling; dimensional analysis; terminal velocity; spherical particles; drag coefficient

check for updates

Citation: Friso, D. Mathematical Modeling of Particle Terminal Velocity for Improved Design of Clarifiers, Thickeners and Flotation Devices for Wastewater Treatment. *Clean Technol.* **2023**, *5*, 921–933. https://doi.org/10.3390/cleantechnol5030046

Academic Editor: Nicolas Kalogerakis

Received: 29 March 2023
Revised: 8 May 2023
Accepted: 13 July 2023
Published: 17 July 2023

1. Introduction

In the management of wastewater, for the purpose of depollution, treatment devices are used, including clarifiers, thickeners, flotation cells and, sometimes, centrifuges. All such devices are based on the separation of solid or flocculated particles present in wastewater, by sedimentation or flotation, using gravity or centrifugation. Among these methods, gravity sedimentation has the advantage of almost negligible energy consumption. For example, a clarifier with a surface area of 2800 m^2 requires an electrical power of just 12 kW, and it thus represents an excellent example of clean technology.

Designs and simulations of these separation processes are based on mathematical modeling of the behavior of solid particles in suspension. Research on the behavior of such particles has been mainly oriented towards the calculation of their terminal velocity, on the hypothesis that the individual particle is spherical, is not disturbed during its motion by the presence of other particles (diluted suspensions) and is immersed in a stationary and infinite fluid.

A possible lack of sphericity is considered by introducing coefficients into the formula for the terminal velocity of the spheres [1–4]. For concentrated suspensions, a number of authors [5–7] have reported that, for mathematical modeling of sedimentation using Kynch's theory, it is always necessary to know the value of the terminal velocity of a single sphere.

It is interesting to note that calculation of particle terminal velocity is a matter of interest in other sectors of engineering and technology, in addition to clean technologies; these include the processing sector (drying, freezing, etc.) and transportation using fluidized beds [8–12]. Scientific researchers have also investigated the flotation [13] and sedimentation of particles immersed in non-Newtonian fluids using relative experimental and/or numerical studies of their terminal velocities [14,15]. For particles of sand and other mineral aggregates found during sedimentation, terminal velocity was recently measured and studied by the authors of [16,17]; for larger particles, the recent determination of terminal velocity by the authors of [18] is also worthy of note. In addition, the calculation of particle terminal velocity has been of interest to researchers studying soil erosion during rainfall [19–21], the settling of bioparticles [22] and the dispersion of polluting particles in the atmosphere [23].

During sedimentation, the spherical particle is subjected to drag resistance, which depends on the unknown terminal velocity v and on the drag coefficient C_d which, in turn, depends on the Reynolds number Re, and, therefore, on the unknown velocity v once again, in a complicated manner. If Re is low, the boundary layer is laminar, and the Stokes formula can be obtained from the equation of dynamics; using this formula, the terminal velocity can be determined. If Re has an intermediate value, the boundary layer is transitional and the drag coefficient has a different relationship with Re; consequently, a different formula is required for calculating terminal velocity. If the value of Re is high, the motion in the boundary layer becomes turbulent; in such cases, a third formula for calculating terminal velocity is required.

The choice of which of the three formulas to use therefore depends on Re, which depends, in turn, on the terminal velocity. In the past, this necessitated a long and tedious trial-and-error procedure. However, the identification of the dimensionless number of Archimedes Ar [24–27], obtained by combining the drag coefficient C_d with Re to eliminate the unknown terminal velocity, has made it possible to speed up the calculation procedure, because Ar depends only on the physical characteristics of the particle and fluid, as well as the effects of gravity or centrifugal acceleration. Basically, Ar is previously determined and is then compared with the limit values which define the typology of the boundary layer. Consequently, the relative formula is used for calculating the terminal velocity.

In more recent times, formulas have also been proposed for the calculation of the drag coefficient $C_d = f(Ar)$ and, thus, the terminal velocity $v = f(Ar)$ as a function of the Archimedes number Ar [28–31]. Some of these are valid for a wide range of Re values, i.e., for any type of boundary layer, from laminar to turbulent. These formulas enable algorithms to be constructed which are useful for the design and simulation of the processes of separation involving Re values which range from less than 1 to above 100,000, because these processes may involve the use of gravity acceleration, as in clarifiers, thickeners and flotation cells, or centrifugal acceleration, as in the centrifuges, where the acceleration can exceed 10,000$\times$ g.

In this study, we aimed to develop a formula $C_d = f(Ar)$ which would be valid for a wide range of Ar or Re values and also, therefore, a formula $v = f(Ar)$, which could be added to existing examples in the literature. We sought also to reduce the level of error with respect to the standard experimental data [32]; to this end, a mathematical modeling was carried out based on a dimensional analysis. Furthermore, and by adopting the same conceptual procedure as for the formula with respect to the Archimedes number, $C_d = f(Ar)$, a formula was also developed to express the drag coefficient as a function of Reynolds number, $C_d = f(Re)$. This was done in order to compare the results obtained with those of other authors which are more numerous for the $C_d = f(Re)$ relationship.

By such means, we could highlight any improvement in accuracy compared to formulas previously reported in the literature.

2. Materials and Methods

2.1. Dimensional Analysis

Table 1 lists the six variables involved in the phenomenon of particle–fluid separation due to the difference in density. For each variable, the link to the dimensions of the primary quantities is also given. Because this is a purely mechanical phenomenon, there are only three primary quantities (length, mass and time); therefore, on the basis of Buckingham's π theorem [33], the phenomenon of separation of solid particles present in a suspension can be described by three dimensionless groups (3 groups = 6 variables—3 primary dimensions).

Table 1. Variables involved in sedimentation.

Variables	Symbol	Dimension
Diameter of the particle	D [m]	L
Terminal velocity	v [m s^{-1}]	L T^{-1}
Acceleration (gravity or centrifugal)	a [m s^{-2}]	L T^{-2}
Fluid density	ρ_f [kg m^{-3}]	M L^{-3}
Particle density—fluid density	$(\rho_p - \rho_f)$ [kg m^{-3}]	M L^{-3}
Viscosity	μ [kg m^{-1} s^{-1}]	M L^{-1} T^{-1}

Each of these dimensionless groups will be of the type

$$\Pi = D^a \cdot v^b \cdot a^c \cdot \rho_f^d \cdot \left(\rho_p - \rho_f\right)^e \cdot \mu^f \tag{1}$$

The corresponding dimensional equation is

$$[\Pi] = [D]^a [v]^b [a]^c \left[\rho_f\right]^d \left[\rho_p - \rho_f\right]^e [\mu]^f \tag{2}$$

where the variables are described in Table 1.

Expressing the dimensions of the variables through those of the primary quantities (Table 1), we have

$$\Pi = L^{a+b+c-3d-3e-f} \cdot M^{d+e+f} \cdot T^{-b-2c-f} \tag{3}$$

Because Π must be dimensionless, the previous expression can be translated into the following homogeneous linear system:

$$\begin{cases} a + b + c - 3d - 3e - f = 0 \\ d + e + f = 0 \\ -b - 2c - f = 0 \end{cases} \tag{4}$$

Because the characteristic of the coefficient matrix of this system is three, the three equations are linearly independent, and the number of unknowns is equal to six, i.e., the same as the number of variables under consideration. Therefore, the system is indeterminate, and the algebraic theory ensures that there are independent solutions whose number is equal to that of the unknowns minus the characteristic of the matrix ($6 - 3 = 3$). Bearing in mind that the solutions in Equation (4) are the exponents to the second member of Equation (1), each of these corresponds to a dimensionless group Π.

By setting $c = e = 0$; $a = 1$; from Equation (4) we obtain: $b = 1$; $d = 1$; $f = -1$; namely, the well-known Reynolds number *Re*, as follows:

$$\Pi_1 = \frac{\rho_f v D}{\mu} = Re \tag{5}$$

The second dimensionless group Π_2 is obtained by setting d = 0; c = e = 1; from Equation (4), we then obtain the following solution: a = 2; b = −1; f = −1; that is,

$$\Pi_2 = \frac{\left(\rho_p - \rho_f\right) \cdot a \cdot D^2}{\mu \cdot v} = Stk \tag{6}$$

In the definition of Stokes number [34,35], i.e., $Stk = \frac{R}{D\mu v}$, R is the drag resistance. According to Newton's law, in conditions of uniform motion, the drag resistance R coincides—except in the case of a multiplicative constant equal to $\pi/6$—with the force of gravity or centrifugal force, net of the buoyancy force, i.e.,: $R = \left(\rho_p - \rho_f\right) \cdot a \cdot D^3$. Therefore, we find that Π_2 coincides with Stk.

By setting c = d = g = 0; a = 1, Equation (4) gives the following solution: b = −1; e = −1; f = 1; this corresponds to the third dimensionless number:

$$\Pi_3 = \frac{\rho_f v^2}{\left(\rho_p - \rho_f\right) \cdot a \cdot D} = \frac{4}{3C_d} \tag{7}$$

We again recall Newton's law relating to uniform motion: $R = C_d \cdot \frac{\pi}{4} \cdot D^2 \cdot \rho_f \cdot \frac{v^2}{2} = \frac{\pi}{6} \cdot \left(\rho_p - \rho_f\right) \cdot a \cdot D^3$. Now, the dimensionless number Π_3 becomes equal to $\frac{4}{3C_d}$, where C_d is the drag coefficient.

The dimensionally correct equation

$$f\left[D, v, a, \rho_f, \left(\rho_p - \rho_f\right), \mu\right] = 0 \tag{8}$$

can now be reduced, thanks to the dimensional analysis, to

$$\Pi_3 = \frac{4}{3C_d} = F(Stk, Re) \tag{9}$$

Both the Stokes number Stk and the Reynolds number Re contain the unknown terminal velocity v, but with their product, v is eliminated, and we obtain the following:

$$Stk \cdot Re = \frac{D^3\left(\rho_p - \rho_f\right) \cdot \rho_f \cdot a}{\mu^2} = Ar \tag{10}$$

This new dimensionless quantity $Stk \cdot Re$ is already known as Archimedes number Ar; however, this has been obtained by other authors [24–26], as the product between the drag coefficient C_d and the square of the Reynolds number ($Ar = \frac{3}{4} C_d \cdot Re^2$). Ultimately, the dimensional analysis suggests looking for a relationship such as this:

$$\frac{4}{3C_d} = f(Ar) \tag{11}$$

2.2. Experimental Data

To make explicit the function *f(Ar)*, experimental data in the form of pairs (C_d, Ar) are needed. In the current study, the data of Lapple–Shepherd [32] were chosen because these are average values of historical data from 17 different authors; for this reason, they are called standard drag curve (SDC) data [3]. These data are in the form of pairs (C_d, Re), but because the following holds: $Ar = \frac{3}{4} C_d \cdot Re^2$, it is easy to transform the pairs (C_d, Re) into (C_d, Ar) (Table 2).

Table 2. Standard drag curve (SDC) data [3,32] for the drag coefficient C_d vs. Reynolds number *Re*. The column on the right shows the calculated value of the Archimedes number *Ar*.

C_d Value from Standard Drag Curve (SDC)	Reynolds Number *Re*	Archimedes Number *Ar*
240	0.1	1.8
80	0.3	5.4
36.5	0.7	13.4
26.5	1	19.9
10.4	3	70.2
5.4	7	198.5
4.1	10	307.5
2.0	30	1350
1.27	70	4667
1.07	100	8025
0.65	300	43,875
0.50	700	183,750
0.46	1000	345,000
0.40	3000	2,700,000
0.39	7000	14,332,500
0.41	10,000	3075×10^4
0.47	30,000	$31{,}725 \times 10^4$
0.50	70,000	$18{,}375 \times 10^5$
0.48	100,000	36×10^8
0.498	200,000	149.4×10^8

To better identify the function $\frac{4}{3C_d} = f(Ar)$, the two dimensionless numbers are logarithmized: $\ln\left(\frac{4}{3C_d}\right) = f(\ln Ar)$, highlighting in this case a function which increases almost monotonically (Figure 1).

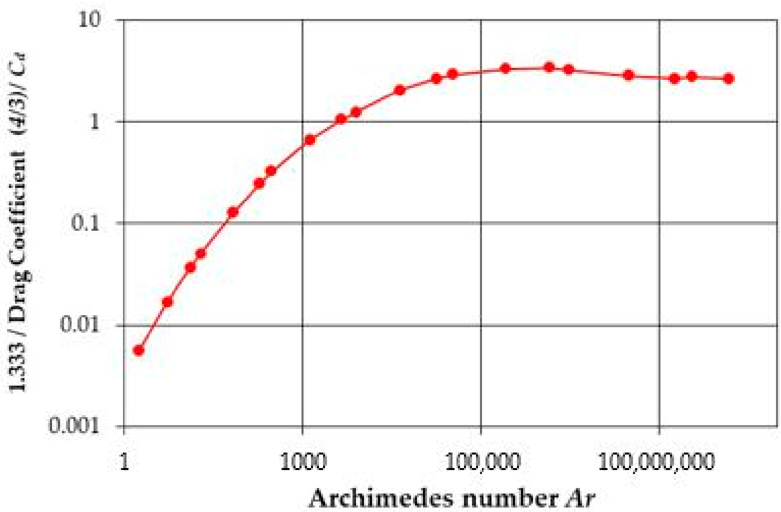

Figure 1. The dimensionless number $(4/3)/C_d$ vs. Archimedes number *Ar*.

3. Results and Discussion

3.1. Formulas $C_d = f(Ar)$ and $v = f(Ar)$

The search for the function $\ln\left(\frac{4}{3C_d}\right) = f(\ln Ar)$ was carried out through a polynomial regression of the SDC experimental data of Table 2 and, therefore, of Figure 1, from which the following equation was obtained:

$$\ln\left(\frac{4}{3C_d}\right) = 0.0000013458 \cdot F^5 - 0.000070578 \cdot F^4 + 0.0021933 \cdot F^3 - 0.065988 \cdot F^2 + 1.13623 \cdot F - 5.83958 \quad (12)$$

where $F = \ln(Ar)$. When R^2 = 0.99991, Equation (12) holds for the following Archimedes range: $1.8 \leq Ar \leq 149.4 \times 10^8$ (Reynolds range: $0.1 \leq Re \leq$ 200,000).

From Equation (12), by collecting the term $F = \ln(Ar)$, we now obtain

$$\begin{aligned}\ln\left(\frac{4}{3C_d}\right) + 5.83958 &= \left\{0.0000013458{\cdot}F^4 - 0.000070578{\cdot}F^3 + 0.0021933{\cdot}F^2 - 0.065988{\cdot}F + 1.13623\right\}\cdot\ln(Ar) \\ &= \ln\left(Ar^{0.0000013458\cdot F^4 - 0.000070578\cdot F^3 + 0.0021933\cdot F^2 - 0.065988\cdot F + 1.13623}\right)\end{aligned} \quad (13)$$

Therefore,

$$\frac{4}{3C_d} = e^{-5.83958}{\cdot}Ar^{0.0000013458\cdot F^4 - 0.000070578\cdot F^3 + 0.0021933\cdot F^2 - 0.065988\cdot F + 1.13623} \quad (14)$$

Finally, the formula that provides the drag coefficient C_d can be stated thus:

$$C_d = 458.18{\cdot}Ar^{-(0.0000013458\cdot F^4 - 0.000070578\cdot F^3 + 0.0021933\cdot F^2 - 0.065988\cdot F + 1.13623)} \quad (15)$$

In Table 3, the C_d values obtained from Equation (15) are compared with the reference experimental values of the SDC (standard drag curve) [32]. To evaluate the accuracy of the formula, the criterion of "relative difference" (RD) is used [3]. This is expressed as a percentage defined as "100 · (∣estimated value—reference data∣)/reference data". The evaluation is then completed by determining the average of these RD values, thus obtaining the mean relative difference (MRD).

Table 3. Drag coefficient C_d estimates calculated with Equation (15) in comparison with standard drag curve (SDC) data [3,32]. The third column shows values of relative difference (RD); among these, the highest value (HRD) is bold and underlined.

C_d Value from Equation (15)	C_d Value from Standard Drag Curve (SDC)	Relative Difference (RD) (%)	Reynolds Number Re	Archimedes Number Ar
240.27	240	0.11	0.1	1.8
80.55	80	0.68	0.3	5.4
36.12	36.5	−1.05	0.7	13.4
26.23	26.5	−1.01	1	19.9
10.40	10.4	0.03	3	70.2
5.41	5.4	0.15	7	198.5
4.22	4.1	2.86	10	307.5
2.03	2.0	1.57	30	1350
1.24	1.27	−2.18	70	4667
1.03	1.07	−3.31	100	8025
0.655	0.65	0.72	300	43,875
0.504	0.50	0.85	700	183,750
0.464	0.46	0.96	1000	345,000
0.401	0.40	0.14	3000	2,700,000
0.397	0.39	1.88	7000	14,332,500
0.406	0.41	−1.03	10,000	3075×10^4
0.456	0.47	−3.03	30,000	$31{,}725 \times 10^4$
0.495	0.50	−1.02	70,000	$18{,}375 \times 10^5$
0.502	0.48	**<u>4.68</u>**	100,000	36×10^8
0.490	0.498	−1.58	200,000	149.4×10^8

The previously reported formulas [28–31] with which it is possible to obtain the Reynolds number as a function of the Archimedes number, $Re = f(Ar)$, were taken from Table 3 of Kalman [36] and are re-presented here in Table 4. From the Archimedes number definition, $Ar = \frac{3}{4}C_d{\cdot}Re^2$, we derived the following formulas: $C_d = \frac{4}{3}\frac{Ar}{Re^2} = \frac{4}{3}\frac{Ar}{[f(Ar)]^2}$

Table 4. Formulas from the literature describing the drag coefficient C_d vs. Archimedes number Ar.

Authors	Year	Formula	Ar Range
Khan–Richardson [28]	1987	$C_d = \frac{4}{3}Ar \cdot \left[2.33 \cdot Ar^{0.018} - 1.53 \cdot Ar^{0.016}\right]^{-2 \cdot 13.3}$	$1.8 \div 353{,}250$
Haider–Levenspiel [29]	1989	$C_d = \frac{4}{3}Ar \cdot \left[\frac{18}{Ar} + \frac{2.412}{4 \cdot Ar^{0.5}}\right]^{-2}$	$1.8 \div 149.4 \cdot 10^8$
Nguyen et al. [30]	1997	$C_d = \frac{4}{3}Ar \cdot \left[\frac{Ar}{18} \cdot \frac{1}{1 + \frac{Ar}{96} \cdot \left(1 + 0.079 \cdot Ar^{0.749}\right)^{-0.755}}\right]^{-2}$	$1.8 \div 353{,}250$
Brown–Lawler, their Equation (37) in [31]	2003	$C_d = \frac{4}{3}Ar \cdot \left[\frac{Ar \cdot \left(22.5 + Ar^{0.682}\right)}{0.0258 \cdot Ar^{1.349} + 2.81 \cdot Ar^{1.015} + 18 \cdot Ar^{0.682} + 405}\right]^{-2}$	$1.8 \div 27 \cdot 10^5$

By comparing the results of the formulas of Table 4 with the experimental data of the standard drag curve (SDC), the mean relative difference (MRD) and standard deviation (SD) were obtained; these are shown in Table 5. The values of the MR and SD of Equation (15) are also shown in the last three lines. In fact, for the Equation (15) the calculation of MRD and SD was carried out in three different ranges of Reynolds numbers, with upper bounds of 1000, 4000 and 200,000, respectively, to make the comparison to other formulas homogeneous. For example, the MRD = 1.44% in the last line is useful for comparison with the MRD = 12.34% of the Haider–Levenspiel formula [29] because the *Re* range is the same.

Table 5. Mean relative difference (MRD) and standard deviation (SD) of the C_d values obtained using Equation (15), compared with the values obtained using the previously published formulas presented in Table 4.

Authors	Year	Mean Relative Difference (MRD) (%)	Standard Deviation (SD) (%)	Ar Range	Re Range
Khan–Richardson [28]	1987	2.24	1.90	$1.8 \le Ar \le 353{,}250$	$0.1 \le Re \le 1000$
Haider–Levenspiel [29]	1989	12.34	8.08	$1.8 \le Ar \le 149.4 \cdot 10^8$	$0.1 \le Re \le 200{,}000$
Nguyen et al. [30]	1997	4.19	2.49	$1.8 \le Ar \le 353{,}250$	$0.1 \le Re \le 1000$
Brown–Lawler, their Equation (37) in [31]	2003	3.57	2.97	$1.8 \le Ar \le 27 \cdot 10^5$	$0.1 \le Re \le 4000$
Present work, Equation (15)	2023	1.22	1.16	$1.8 \le Ar \le 353{,}250$	$0.1 \le Re \le 1000$
Present work, Equation (15)	2023	1.17	1.13	$1.8 \le Ar \le 27 \cdot 10^5$	$0.1 \le Re \le 4000$
Present work, Equation (15)	2023	1.44	1.23	$1.8 \le Ar \le 149.4 \cdot 10^8$	$0.1 \le Re \le 200{,}000$

In all cases, the proposed Equation (15) results in the best fitting of the standard drag curve SDC.

Using Equation (15), and recalling the definition of the third dimensionless number of Equation (7), from which we obtain this expression: $C_d = \frac{4}{3}\frac{\left(\rho_p - \rho_f\right) a \cdot D}{\rho_f v^2}$, it is easy to derive the formula for the terminal velocity v:

$$v = \left[\frac{\left(\rho_p - \rho_f\right) a \cdot D}{\rho_f} 0.00291 \cdot Ar^{(0.0000013458 \cdot F^4 - 0.000070578 \cdot F^3 + 0.0021933 \cdot F^2 - 0.065988 \cdot F + 1.13623)}\right]^{1/2} \tag{16}$$

3.2. Formula $C_d = f(Re)$

Given the usefulness of also having a formula for the drag coefficient vs. the Reynolds number $C_d = f(Re)$, we used the same regression procedure implemented for Equation (15), $C_d = f(Ar)$, and starting from the SDC data in the first and second columns of Table 2, obtained the following result:

$$\ln\left(\frac{1}{C_d}\right) = 0.000037447 \cdot G^5 - 0.00066989 \cdot G^4 + 0.0016779 \cdot G^3 - 0.033243 \cdot G^2 + 0.86961 \cdot G - 3.27 \tag{17}$$

where $G = \ln(Re)$. When R^2 = 0.99990, Equation (17) holds for the following Reynolds number range: $0.1 \leq Re \leq 200{,}000$.

From Equation (17), collecting the term $G = \ln(Re)$, and proceeding as we did when obtaining Equation (15), but without reporting the intermediate steps, we then obtain

$$C_d = 26.31 \cdot Re^{-(0.000037447 \cdot G^4 - 0.00066989 \cdot G^3 + 0.0016779 \cdot G^2 - 0.033243 \cdot G + 0.86961)} \tag{18}$$

Recalling Stokes' law [37], i.e., Drag Resistence $= R = 3 \cdot \pi \cdot D \cdot \mu \cdot v = \boldsymbol{C_d} \cdot \pi D^2/4 \cdot \rho \cdot v^2/2 \rightarrow C_d = 24/Re$, which is valid for $Re \leq 0.5$, the term $\boldsymbol{C_d} = 24/Re$ can be highlighted in Equation (18):

$$C_d = \frac{24}{Re} \cdot 1.0963 Re^{-(0.000037447 \cdot G^4 - 0.00066989 \cdot G^3 + 0.0016779 \cdot G^2 - 0.033243 \cdot G - 0.13039)} \tag{19}$$

Equation (19) therefore takes the form of Stokes' law $C_d = 24/Re$, multiplied by a correction factor, similarly to the formulas of some authors in the literature. In Table 6, the C_d values obtained from Equation (19) are reported in the first column and are compared with the experimental values of the standard drag curve (SDC) in the second column. The relative differences (RDs) between the C_d values obtained from Equation (19) and those of the SDC data are presented in the third column.

Table 6. Estimates of drag coefficient C_d calculated with Equation (19), compared with standard drag curve (SDC) data from [3,32]. The third column shows the relative differences (RDs); among these, the highest value (HRD) is bold and underlined.

C_d Value from Equation (19)	C_d Value from Standard Drag Curve (SDC)	Relative Difference (RD) (%)	Reynolds Number *Re*	Archimedes Number *Ar*
242.34	240	0.98	0.1	1.8
79.01	80	−1.23	0.3	5.4
36.03	36.5	−1.27	0.7	13.4
26.31	26.5	−0.71	1	19.9
10.52	10.4	1.17	3	70.2
5.47	5.4	1.36	7	198.5
4.22	4.1	2.93	10	307.5
2.02	2.0	1.03	30	1350
1.24	1.27	−2.55	70	4667
1.03	1.07	−3.68	100	8025
0.646	0.65	−0.62	300	43,875
0.502	0.50	0.32	700	183,750
0.464	0.46	0.90	1000	345,000
0.406	0.40	1.44	3000	2,700,000
0.403	0.39	3.32	7000	14,332,500
0.410	0.41	0.0	10,000	3075×10^4
0.452	0.47	<u>**−3.85**</u>	30,000	$31{,}725 \times 10^4$
0.488	0.50	−2.49	70,000	$18{,}375 \times 10^5$
0.496	0.48	3.34	100,000	36×10^8
0.487	0.498	−2.19	200,000	149.4×10^8

In the literature, numerous relationships have been reported between the drag coefficient and the Reynolds number, for values of the latter up to 200,000; formulas expressing these relationships are shown in Table 7.

Figure 2 shows the standard drag curve (SDC), together with the drag curve of Equation (19) and the drag curves obtained with the formulas from the literature shown in Table 7, all of which are valid for Reynolds number values from 0.1 to 200,000.

Table 7. Formulas from the literature describing the drag coefficient C_d vs. Reynolds number *Re*. All formulas are valid in the Reynolds number range from 0.1 to 200,000.

Authors	Year	Formula
El Hasadi–Padding, their Equation (11) [4]	2022	$C_d = 3.286 + \frac{24.205}{Re} - 0.818 \cdot G + 0.064 \cdot G^2 - 0.000107 \cdot G^4$, where: $G = \ln Re$
Hongli et al.their Equation (25) in [38]	2015	$C_d = \frac{24}{Re} \cdot \left(1 + \frac{3}{16} Re\right)^{0.635} + 0.468 \cdot \sin^2 \alpha$ where: $\alpha = \left[1 - \exp\left(-3.24x^2 + 8x^4 - 6.5x^5\right)\right] \frac{\pi}{2}$ and $x = 0.1 \cdot \ln(1 + Re)$
Clift–Gauvin [39]	1970	$C_d = \frac{24}{Re} \cdot \left(1 + 0.15 \cdot Re^{0.687}\right) + \frac{0.42}{1 + \frac{42,500}{Re^{1.16}}}$
Brown–Lawler, their Equation (19) in [31]	2003	$C_d = \frac{24}{Re} \cdot \left(1 + 0.15 \cdot Re^{0.681}\right) + \frac{0.407}{1 + \frac{8710}{Re}}$
Cheng [40]	2009	$C_d = \frac{24}{Re} \cdot (1 + 0.27 \cdot Re)^{0.43} + 0.47 \cdot \left[1 - \exp\left(-0.04 \cdot Re^{0.38}\right)\right]$
Terfous et al. [41]	2013	$C_d = 2.6689 + \frac{21.683}{Re} + \frac{0.31}{Re^2} - \frac{10.616}{Re^{0.1}} + \frac{12.216}{Re^{0.2}}$
Turton–Levenspiel [42]	1986	$C_d = \frac{24}{Re} \cdot \left(1 + 0.173 \cdot Re^{0.657}\right) + \frac{0.413}{1 + \frac{16,300}{Re^{1.09}}}$
Haider–Levenspiel [29]	1989	$C_d = \frac{24}{Re} \cdot \left(1 + 0.1806 \cdot Re^{0.6459}\right) + \frac{0.4251}{1 + \frac{6880.95}{Re}}$
Kahn–Richardson [28]	1987	$C_d = \left(2.25 \cdot Re^{-0.31} + 0.36 \cdot Re^{0.06}\right)^{3.45}$
Kaskas [43]	1970	$C_d = \frac{24}{Re} + \frac{4}{Re^{0.5}} + 0.4$
Ganser [44]	1993	$C_d = \frac{24}{Re} \cdot \left(1 + 0.1118 \cdot Re^{0.6567}\right) + \frac{0.4305}{1 + \frac{3305}{Re}}$
Brauer [45]	1973	$C_d = \frac{24}{Re} + \frac{3.73}{Re^{0.5}} - \frac{4830 \cdot Re^{0.5}}{1 - 300,000 \cdot Re^{1.5}} + 0.49$
Barati et al., their Equation (22) in [46]	2014	$C_d = 5.4856 \cdot 10^9 \cdot \tanh\left(\frac{4.3779 \cdot 10^9}{Re}\right) + 0.0709 \cdot \tanh\left(\frac{700.6574}{Re}\right) + 0.3894 \cdot \tanh\left(\frac{70.1539}{Re}\right) - 0.1198 \cdot \tanh\left(\frac{7429.0843}{Re}\right) + 1.7174 \cdot \tanh\left(\frac{9.9851}{Re + 2.3384}\right) + 0.4744$

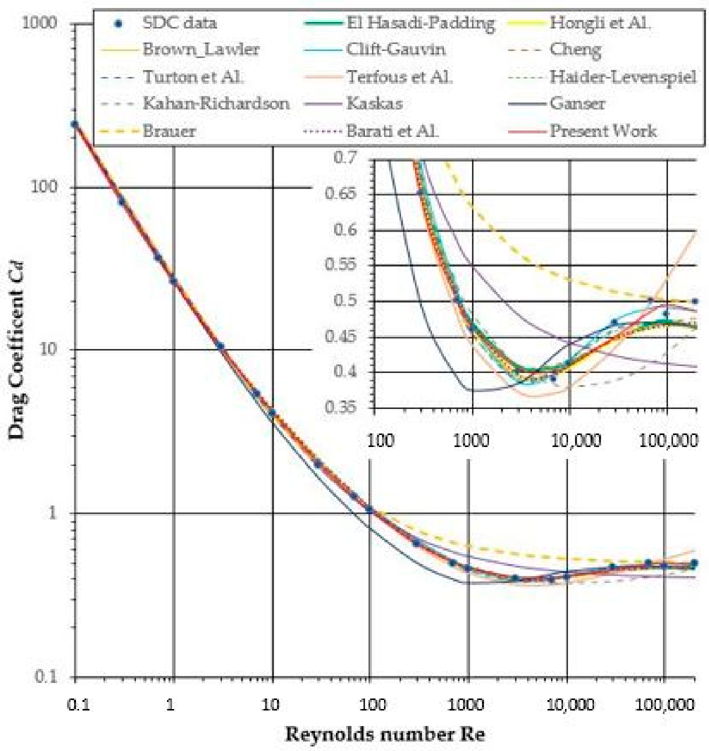

Figure 2. Comparison between the drag coefficients predicted by Equation (19) and by the formulas from the literature described in Table 7: Brown-Lawler [31], Tourton et al. [42], Kahn-Richardson [27], Brauer [45], El Hasadi-Padding [4], Clift-Gauvin [39], Terfous et al. [41], Kaskas [43], Barati et al. [46], Hongli et al. [38], Cheng [40], Haider-Levenspiel [29], Ganser [44]. Blue point symbols indicate the experimental values of the standard drag curve (SDC).

By comparing the results obtained using Equation (19) and the formulas in Table 7 with the data of the standard drag curve (SDC), the mean relative differences (MRDs) and standard deviations (SDs) were obtained; these values are shown in Table 8. Note that Equation (19) produces the highest level of accuracy, with an MRD of 1.77% and an SD of 1.17%.

Table 8. Mean relative difference (MRD), standard deviation (SD) and highest relative difference (HRD) of the C_d values versus the standard drag curve (SDC), obtained with the Equation (19) and with the literature formulas described in Table 7. Equations are valid in the Reynolds number range from 0.1 to 200,000.

Authors	Year	Mean Relative Difference (MRD) (%)	Stand. Deviat. (SD) (%)	Highest Relative Difference (HRD) (%)	Reynolds Number *Re* at the HRD
SDC data [3,32]	1940				
Present work, Equation (19)	2023	1.77	1.17	−3.85	30,000
El Hasadi-Padding their Equation (11) [4]	2022	2.24	1.99	−7.30	200,000
Hongli et al. their Equation (25) [38]	2015	2.51	2.27	−7.13	70,000
Barati et al. their Equation (22) [46]	2014	2.67	2.25	−7.31	70,000
Clift-Gauvin [39]	1970	2.68	1.70	6.56	0.3
Brown-Lawler their Equation (19) [31]	2003	2.76	2.30	−7.04	70,000
Cheng [40]	2009	2.98	2.01	−7.13	70,000
Terfous et al. [41]	2013	3.92	4.93	20.52	200,000
Turton-Levenspiel [42]	1986	3.93	1.97	7.84	0.3
Haider-Levenspiel [29]	1989	4.06	2.17	8.30	0.3
Kahn-Richardson [28]	1987	4.88	4.97	−17.39	70,000
Kaskas [43]	1970	9.70	6.43	20.26	3000
Ganser [44]	1993	10.22	8.35	−24.79	100
Brauer [45]	1973	12.63	14.66	41.53	3000

The formula of Barati et al. [46], described in Table 7, presents the greatest complexity, with a total of 12 numerical coefficients. This is because the equation was obtained to represent the values of the drag coefficient C_d for *Re* values between 0.002 and 200.000. El Hasadi–Padding's formula [4] can also be used for *Re* values of less than 0.1, as low as $Re = 0.002$.

Therefore, for a more homogeneous comparison between Barati's Equation (22) [46], El Hasadi-Padding's Equation (11) [4], and our Equation (19), the latter was re-obtained with the regression, including also the experimental values of the C_d-*Re* pairs, found in [46], with *Re* values between 0.002 and 0.1 included. By such means, Equation (19), for $0.002 \leq Re \leq 200{,}000$, becomes

$$C_d = \frac{24}{Re} \cdot 1.12706 \cdot Re^{-(0.000011813 \cdot G^4 - 0.000038857 \cdot G^3 - 0.0028857 \cdot G^2 - 0.027371 \cdot G - 0.10251)} \tag{20}$$

By comparing the results of Equation (20), Barati's Equation (22) [46] and El Hasadi–Padding's Equation (11) [4] described in Table 7 with the data of the standard drag curve (SDC), the mean relative differences (MRDs) and standard deviations (SDs) were obtained; these values are shown in Table 9.

Table 9. Mean relative difference (MRD), standard deviation (SD) and highest relative difference (HRD) of the C_d values versus the standard drag curve (SDC), obtained with Equation (20), with Barati's Equation (22) [46] and with El Hasadi–Padding's Equation (11) [4] described in Table 7. Equations are valid in the Reynolds number range from 0.002 to 200,000.

Authors	Year	Mean Relative Difference (MRD) (%)	Stand. Deviat. (SD) (%)	Highest Relative Difference (HRD) (%)	Reynolds Number *Re* at the HRD
SDC data [3,46]	1940				
Present work, Equation (20)	2023	2.20	1.53	−6.36	30,000
Barati et al., their Equation (22) [46]	2014	2.12	2.22	−7.31	70,000
El Hasadi–Padding, their Equation (11) [4]	2022	2.34	1.77	−7.30	200,000

Note that the three formulas produce similar levels of accuracy, with a slightly better MRD value for Barati's formula (2.12% versus 2.20% and 2.34%) and a slightly better SD value for Equation (20) of the current study (1.53% versus 2.22% and 1.77%). However, Equation (20) involves only six coefficients, i.e., half the number of Barati's formula.

4. Conclusions

Because solid/liquid separation, especially when using gravity, involves negligible energy consumption and can therefore be regarded as an excellent clean technology, the availability of formulas for calculating terminal velocity for a single spherical particle is essential for realizing mathematical modeling useful for the design and control of wastewater separators as clarifiers, thickeners, flotation devices and centrifuges; in fact, the velocities of spherical and non-spherical particles can easily be connected through coefficients, and the co-presence of other particles can be described by Kynch's theory, which in any case makes use of the value of the terminal velocity of a single sphere.

Therefore, a precise prediction of the terminal velocity of spherical solid particles in wastewater as suspensions is indispensable for any mathematical description of the separation processes. Because the separation processes can be performed using gravity acceleration, as with clarifiers and/or thickeners and/or flotation devices; or centrifugal acceleration, as with continuous decanter centrifuges and/or disk centrifuges where the acceleration can exceed 10,000$\times$ g, the Reynolds numbers of particles can be low, as happens with small particles and with gravity acceleration, or high (or very high) with large particles and/or centrifugal acceleration.

Because the drag resistance of the sphere immersed in the liquid depends on the terminal velocity v and on the drag coefficient C_d, which depends, in turn, on the Reynolds number Re, and therefore again on the unknown velocity v, the use of classical relations between the drag coefficient and the Reynolds number makes calculating the terminal velocity awkward. It is preferable to have a relationship between the drag coefficient and the Archimedes number Ar which does not contain the terminal velocity.

There are already formulas in the literature for calculating the drag coefficient as a function of Archimedes number, i.e., $C_d = f(Ar)$, with which the formula for calculating the terminal speed, i.e., $v = f(Ar)$ can easily be written. Unfortunately, such formulas are few in number and only one is valid for a wide range of Ar which corresponds to the desired range of $0.1 \leq Re \leq 200{,}000$. Furthermore, this particular formula does not offer accurate results.

A new formula, $C_d = f(Ar)$ (Equation (15)), was therefore developed through dimensional analysis. The formula is valid from a minimum Reynolds number value of 0.1 to a maximum value of 200,000. Using this formula, the mean relative difference MRD compared to the standard drag curve (SDC) data is only 1.44%. In comparison, the best previous formula that is valid always for $0.1 \leq Re \leq 200{,}000$ gives an MRD of 12.34%.

The development of Equation (15), with its use of dimensionless numbers in the form of logarithms, and the high accuracy obtained with this method, led us to think that an equally accurate formula for the drag coefficient could also be obtained with respect to a Reynolds number, i.e., $C_d = f(Re)$ (Equation (19)). Using this formula, the results were again encouraging in terms of accuracy, with an MRD of 1.77%, that is, a value lower than that of all the formulas in the literature, again for a Reynolds range of $0.1 \leq Re \leq 200{,}000$.

The result obtained with Equation (15), and the consequent Equation (16) for the calculation of the terminal velocity, allows us to continue our research to apply this formula within Kynch's theory [5] and thereby obtain a new mathematical model [47] for the design of clarifiers, thickeners, flotation devices and centrifuges, within an overall orientation towards energy saving [48].

Funding: This research received no external funding.

Institutional Review Board Statement: Not applicable.

Informed Consent Statement: Not applicable.

Data Availability Statement: The data presented in this study are contained within the article.

Conflicts of Interest: The author declares no conflict of interest.

Abbreviations

SDC	Standard drag curve
RD	Relative difference
MRD	Mean relative difference
HRD	Highest relative difference
SD	Standard deviation

References

1. Ganguly, U.P. On the prediction of terminal settling velocity of solids in-solid systems. *Int. J. Miner. Process.* **1990**, *29*, 235–247. [CrossRef]
2. Tsakalakis, K.G.; Stamboltzis, G.A. Prediction of the settling velocity of irregularly shaped particles. *Miner. Eng.* **2001**, *14*, 349–357. [CrossRef]
3. Goossens, W.R.A. Review of the empirical correlations for the drag coefficient of rigid spheres. *Powder Technol.* **2019**, *352*, 350–359. [CrossRef]
4. El Hasadi, Y.M.F.; Padding, J.T. Do logarithmic terms exist in the drag coefficient of a single sphere at high Reynolds numbers? *Chem. Eng. Sci.* **2023**, *265*, 118195. [CrossRef]
5. Kynch, G.J. A theory of sedimentation. *Trans. Faraday Soc.* **1952**, *48*, 166–176. [CrossRef]
6. Richardson, J.F.; Zaki, W.N. Sedimentation and fluidization: Part I. *Trans. Inst. Chem. Eng.* **1954**, *32*, S82–S100.
7. Chang, D.; Lee, T.; Jang, Y.; Kim, M.; Lee, S. Non colloidal sedimentation compared with Kynch theory. *Powder Technol.* **1997**, *92*, 81–87. [CrossRef]
8. Sun, Z.; Zhu, J. Demarcation on a new conventional circulating fluidization regime in liquid-solids fluidization via experimental and numerical studies. *Chem. Eng. J.* **2021**, *412*, 128578. [CrossRef]
9. Reguła, T.; Frączek, J.; Fitas, J. A Model of Transport of Particulate Biomass in a Stream of Fluid. *Processes* **2021**, *9*, 5. [CrossRef]
10. do Nascimento, O.L.; Reay, D.A.; Zivkovic, V. Solid Circulating Velocity Measurement in a Liquid–Solid Micro-Circulating Fluidised Bed. *Processes* **2020**, *8*, 1159. [CrossRef]
11. Alghamdi, Y.A.; Peng, Z.; Luo, C.; Almutairi, Z.; Moghtaderi, B.; Doroodchi, E. Systematic Study of Pressure Fluctuation in the Riser of a Dual Inter-Connected Circulating Fluidized Bed: Using Single and Binary Particle Species. *Processes* **2019**, *7*, 890. [CrossRef]
12. Lucena-Thomas, J.P.D.; Boonprasirt, P.; Luetchford, K.; De Bank, P.; Ellis, M. Bed expansion properties of tissue engineering particles in a fluidised bed bioreactor. *Biochem. Eng. J.* **2020**, *160*, 107632. [CrossRef]
13. Chen, Y.; Wang, L.; Chang, H.; Zhang, Q. A review of drag coefficient models in gas-liquid two-phase flow. *ChemBioEng Rev.* **2023**, *10*, 311–325. [CrossRef]
14. Maiti, S.B.; Bar, N.; Das, S.K. Terminal settling velocity of solids in the pseudoplastic non-Newtonian liquid system—Experiment and ANN modeling. *Chem. Eng. J. Adv.* **2021**, *7*, 100136. [CrossRef]
15. Trofa, M.; D'Avino, G. Sedimentation of Fractal Aggregates in Shear-Thinning Fluids. *Appl. Sci.* **2020**, *10*, 3267. [CrossRef]
16. Ma, X.; Ji, G.; Li, Z.; Ju, G. An Improved Model for Predicting the Drag Coefficient and Terminal Settling Velocity of Natural Sands in Newtonian Fluid. *Processes* **2022**, *10*, 1579. [CrossRef]
17. Moruzzi, R.B.; Campos, L.C.; Sharifi, S.; Grava da Silva, P.; Gregory, J. Nonintrusive investigation of large Al-kaolin fractal aggregates with slow settling velocities. *Water Res.* **2020**, *185*, 116287. [CrossRef]
18. Nikolaev, A.A. The Physical Characterization and Terminal Velocities of Aluminium, Iron and Plastic Bottle Caps in a Water Environment. *Recycling* **2022**, *7*, 28. [CrossRef]
19. Jang, S.; Lim, K.-S.S.; Ko, J.; Kim, K.; Lee, G.; Cho, S.-J.; Ahn, K.-D.; Lee, Y.-H. Revision of WDM7 Microphysics Scheme and Evaluation for Precipitating Convection over the Korean Peninsula. *Remote Sens.* **2021**, *13*, 3860. [CrossRef]
20. Naves, J.; Anta, J.; Suárez, J.; Puertas, J. Development and Calibration of a New Dripper-Based Rainfall Simulator for Large-Scale Sediment Wash-Off Studies. *Water* **2020**, *12*, 152. [CrossRef]
21. Talchabhadel, R.; Nakagawa, H.; Kawaike, K.; Prajapati, R. Evaluating the rainfall erosivity (R-factor) from daily rainfall data: An application for assessing climate change impact on soil loss in Westrapti River basin, Nepal. *Model. Earth Syst. Environ.* **2020**, *6*, 1741–1762. [CrossRef]
22. Liu, X.; Wang, J.; Chai, Z.; Min, F.; Jiang, X.; Zhu, K.; Dai, J. New model for predicting terminal settling velocity and drag coefficient of the Oncomelania. *Front. Environ. Sci.* **2022**, *10*, 1051392. [CrossRef]
23. Takemi, T.; Poulidis, A.P.; Iguchi, M. High–Resolution Modeling of Airflows and Particle Deposition over Complex Terrain at Sakurajima Volcano. *Atmosphere* **2021**, *12*, 325. [CrossRef]
24. Kalman, H. Role of Reynolds and Archimedes numbers in particle-fluid flows. *Rev. Chem. Eng.* **2020**, *38*, 149–165. [CrossRef]
25. Goossens, W.R.A. Classification of fluidized particles by Archimedes number. *Powder Technol.* **1998**, *98*, 48–53. [CrossRef]

26. Loncin, M.; Merson, R.L. *Food Engineering: Principles and Selected Application*, 1st ed.; Accademic Press: New York, NY, USA, 1979; pp. 94–97.
27. Mafart, P.; Belliard, E. *Genie Industriel Alimentaire*, 2nd ed.; Lavoisier: Paris, France, 2004; Volume 2, p. 81.
28. Khan, A.R.; Richardson, J.F. The resistance to motion of a solid sphere in a fluid. *Chem. Eng. Commun.* **1987**, *62*, 135–150. [CrossRef]
29. Haider, A.; Levenspiel, O. Drag coefficient and terminal velocity of spherical and nonspherical particles. *Powder Technol.* **1989**, *58*, 63–70. [CrossRef]
30. Nguyen, A.V.; Stechemesser, H.; Zobel, G.; Schulze, H.J. An improved formula for terminal velocity of rigid spheres. *Int. J. Miner. Process.* **1997**, *50*, 53–61. [CrossRef]
31. Brown, P.P.; Lawler, D.F. Sphere Drag and Settling Velocity Revisited. *J. Environ. Eng. ASCE* **2003**, *129*, 222–231. [CrossRef]
32. Lapple, C.E.; Shepherd, C.B. Calculation of particle trajectories. *Ind. Eng. Chem.* **1940**, *32*, 605–617. [CrossRef]
33. Perry, R.H.; Green, D.W. *Chemical Engineers' Handbook*, 6th ed.; McGraw-Hill: Singapore, 1984; Chapter 5; p. 67.
34. Molerus, O. Fluid mechanics in term of eigen parameter. Part 1: Fundamentals. *Chem. Eng. Sci.* **2000**, *55*, 1171–1177. [CrossRef]
35. Gomez, C.O.; Maldonado, M. Modelling Bubble Flow Hydrodynamics: Drift-Flux and Molerus Models. *Minerals* **2022**, *12*, 1502. [CrossRef]
36. Kalman, H.; Matana, E. Terminal velocity and drag coefficient for spherical particles. *Powder Technol.* **2022**, *396*, 181–190. [CrossRef]
37. Stokes, G. On the effect of the internal friction of fluids on the motion of pendulums. *Trans. Camb. Phillosophical Soc.* **1851**, *9*, 38–39.
38. Hongli, Y.; Minqiang, F.; Airong, L.; Lianping, D. General formulas for drag coefficient and settling velocity of sphere based on theoretical law. *Int. J. Min. Sci. Technol.* **2015**, *25*, 219–223. [CrossRef]
39. Clift, R.; Gauvin, W.H. Motion of entrained particles in gas streams. *Proc. Chem.* **1970**, *70*, 14. [CrossRef]
40. Cheng, N.-S. Comparison of formulas for drag coefficient and settling velocity of spherical particles. *Powder Technol.* **2009**, *189*, 395–398. [CrossRef]
41. Terfous, A.; Hazzab, A.; Ghenaim, A. Predicting the drag coefficient and settling velocity of spherical particles. *Powder Technol.* **2013**, *239*, 12–20. [CrossRef]
42. Turton, R.; Levenspiel, O. A short note on the drag correlation for spheres. *Powder Technol.* **1996**, *47*, 83–86. [CrossRef]
43. Kaskas, A.A. Schwarmgeschwindigkeit in Mehrkornsuspensionen am Beispiel der Sedimentation. Ph.D. Dissertation, TU Berlin, Berlin, Germany, 1970.
44. Ganser, G.H. A rational approach to drag prediction of spherical and nonspherical particles. *Powder Technol.* **1993**, *77*, 143–152. [CrossRef]
45. Brauer, H. Momentum, mass, and heat-transfer through boundary surface of spherical-particles. *Chem. Ing. Tech.* **1973**, *45*, 1099–1103. [CrossRef]
46. Barati, R.; Neyshabouri, S.A.A.S.; Ahmadi, G. Development of empirical models with high accuracy for estimation of drag coefficient of flow around a smooth sphere: An evolutionary approach. *Powder Technol.* **2014**, *257*, 11–19. [CrossRef]
47. Friso, D. A new mathematical model for food thermal process prediction. *Model. Simul. Eng.* **2013**, *569473*, 21. [CrossRef]
48. Friso, D. Energy saving with total energy system for cold storage in Italy: Mathematical modeling and simulation, exergetic and economic analysis. *Appl. Math. Sci.* **2014**, *8*, 6529–6546. [CrossRef]